ELSEVIER

International Journal of Mass Spectrometry 176 (1998) 63–76

International Journal of Mass Spectrometry

Details of the measurement of rare earth and other trace element abundances by secondary ion mass spectrometry

A.J. Fahey

Chemical Science and Technology Laboratory, National Institute of Standards and Technology, Gaithersburg, MD 20899, USA

Received 6 June 1997; accepted 3 December 1997

Abstract

Details of a method for quantitative measurement of rare earth element (REE) abundances by secondary ion mass spectrometry are presented. The specifics of the multipass deconvolution algorithm are given. Direct measurements of the ratios of REE to REE oxide ion signals (η_i) as a function of energy are shown and investigated. The η_i are important quantities used to determine the intensities of the heavy REE ion signals. Relative sensitivity factors for the REE are given for silicate and sulfide minerals and a comparison of measured relative sensitivity factors among three laboratories is shown. The occurrence of artifacts in the analysis is also discussed. (Int J Mass Spectrom 176 (1998) 63–76) © 1998 Elsevier Science B.V.

Keywords: Rare earth elements; Quantitative secondary ion mass spectrometry

1. Introduction

The determination of rare earth element (REE) and other trace element abundances by secondary ion mass spectrometry (SIMS) was investigated and pioneered by several workers [1–4]. REE abundance measurements by SIMS have become a widespread and useful technique employed in studies addressing problems from terrestrial geology to meteoritics (e.g. see discussions in Ireland [5]).

This work is primarily concerned with the method for REE measurements by SIMS first presented by Zinner and Crozaz [4]. The details of, as well as changes to, the algorithm for deconvolution of the ion signals to derive elemental abundances and some of the analytical details have remained unpublished, even though the method is reasonably well known. Although the general outline of analysis has not changed appreciably since that presented by Zinner and Crozaz [4], the specifics of the deconvolution generally used have evolved. In addition, details of the data acquisition used here are somewhat different than those used by Zinner and Crozaz [4], and calibrations have been obtained for numerous mineral matrices for their REE sensitivity factors since the initial work of Zinner and Crozaz [4] (see e.g. [6–11]). Some trace elements other than the REE have also been measured and compared against references in a number of matrices.

2. Measurements of REEs

Before the use of SIMS for REE abundance measurements, the two most widely used methods were neutron activation and mass spectrometric isotope dilution. Generally these techniques require a few milligrams of sample but have occasionally been used

PII S1387-3806(98)14006-X

to analyze microgram quantities. Neutron activation analysis is done on a whole rock without chemical separation (instrumental neutron activation analysis) or on the chemically separated REE fraction (radiochemical neutron activation analysis). The elements La, Ce, Nd, Sm, Eu, Tb, Dy, Yb, and Lu can be measured at the microgram per gram level to an uncertainty of ~2%.

Mass spectrometric isotope dilution is very sensitive and has low uncertainty [12] (1% to 2% for most REE). The REE must be chemically separated into light and heavy elements to reduce oxide interferences. All of the REE except Pr, Tb, Ho, and Tm, which have only one stable isotope, can be analyzed.

SIMS has been used to measure REE abundances to the microgram per gram level in nanogram quantities of material. The uncertainty of the measurements has typically been ~10% to 20%. Absolute abundance accuracy has been a limitation of the SIMS technique. In addition, when abundances of the light REE are much greater than those of the heavy REE, it is difficult to obtain accurate abundances for the heavy REE because of large oxide interferences. A brief overview of applications of SIMS quantitative analysis to geochemistry is given by Ireland [5].

3. Experimental

The SIMS instrument used for this study was a CAMECA (Cameca, Paris) ims-4f.* Samples were mounted in epoxy, ground flat, given a final polish with 3-μm diamond paste, and coated with carbon or gold. Analyses were performed at a secondary extraction voltage of +4.5 keV and an incident 17 keV O^- beam of ~3 nA. The imaged field was 150 μm in diameter, and a 400-μm field aperture and a 150-μm contrast aperture were used.

The measurement of REE abundances is made under conditions of energy filtering to eliminate complex molecular interferences [4]. A sample voltage offset of −80 V is used with an energy window of 30 eV. The magnet is sequentially cycled through a series of masses from 15.5 u to 238 u. Typically 10 to 30 cycles through the sequence produces 10% counting statistics precision for most of the ion signals. A count time of 1 s was used for the lighter, major elements and 2 to 3 s for the REE and other trace elements.

3.1. Energy centering

To employ energy filtering effectively, the "zero point" of the energy distribution must be well known so that compensation can be made for the effects of sample charging. Fig. 1 shows the energy distributions of Si^+, Ca^+, La^+, Eu^+, Lu^+, and LaO^+ measured with an energy bandpass of 30 eV. Elemental ion signals, such as those from Si and La, are more intense at high energies than molecular species, such as LaO (Fig. 1). In addition, the more complex the molecular ion species, the less intense is the ion signal at higher energies (an example is given in Ireland [5]). During measurements of trace element abundances, the signal strength of the trace elements themselves is too low to determine the position of the energy distribution accurately. To increase the sensitivity to trace elements, the primary beam current is often high (~3 to 10 nA), and the signals from the major elements are too high to measure on the electron multiplier. A minor isotope of a normalizing element can sometimes be used, or another element with a relatively low signal can be used to set the energy offset. Oxygen usually provides an intense enough ion beam at $m/z = 16$ to determine the position of the energy distribution without saturating the electron multiplier in the process.

Before a measurement, the energy slit of the spectrometer is opened to 30 or 40 eV. Initial positioning of the energy slit is performed on a conducting sample so that sample charging is not an issue. The secondary ion beam is centered in the spectrometer lens by adjusting the electrostatic analyzer voltages. The energy slit is then closed to a very narrow band

*Certain commercial equipment, instruments, or materials are identified in this article to adequately specify the experimental procedure. Such identification does not imply recommendation or endorsement by the National Institute of Standards and Technology, nor does it imply that the materials or equipment identified are necessarily the best available for the purpose.

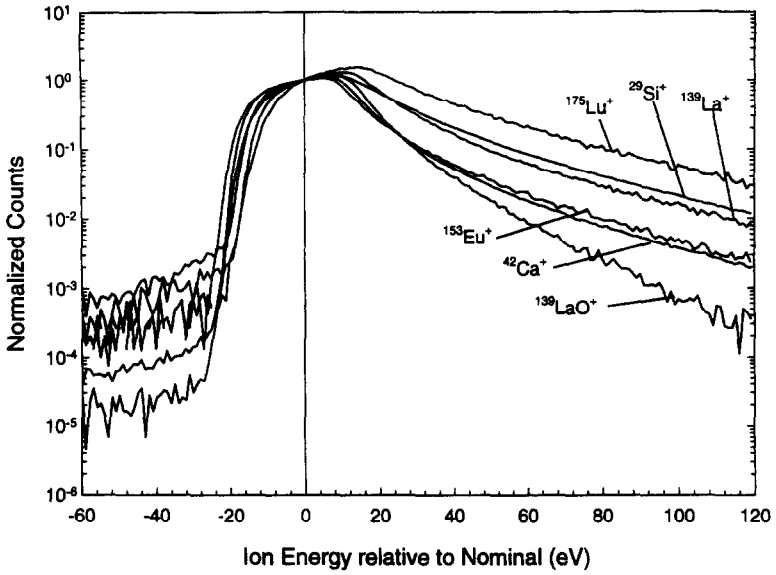

Fig. 1. Energy distribution of secondary positive ions is plotted. Data are normalized for each curve to the counts at zero volts offset. Energy window was set to 30 eV and the nominal ion energy was 4.5 keV.

pass, and its position is adjusted so that the maximum signal is observed. The slit is then opened to 30 eV. The slit is repositioned so that the voltage at which the intensity drops to 10% of the maximum on the low energy edge of the distribution is approximately 1/2 of the slit width (+15 V sample offset). Because the energy distribution is not the same for all elements, one element, $^{27}Al^+$, is always used for this adjustment. When energy filtering is not used (a sample offset of 0 V), ions with energies from a relatively flat part of the distribution will be accepted into the mass spectrometer, reducing the sensitivity to small changes in charging conditions. If the spectrometer were configured to accept ions around the maximum of the distribution, small changes in charging conditions could result in relatively large variations in the relative sensitivities for different elements. When energy filtering is used, as in REE measurements, this procedure determines the position of the energy slit. Fig. 2 shows portions of the energy distributions for Si, Ca, La, Eu, and Lu from 70 to 90 eV normalized to the counts at 80 eV for each element. There is little variation in the relative signals for the elements shown in Fig. 2 in the region of 80 eV, the energy at which analyses are usually performed. Thus, small changes in charging conditions will have little effect on the relative sensitivity factors.

During a measurement on an insulating sample the position of the 10% edge is monitored and the sample voltage adjusted to keep the position fixed to within 0.5 V. This check is usually performed every 5 to 10 cycles through the masses being measured. Typically 5 points on the energy distribution are measured, although the algorithm allows the number of points to vary, and a memory of the previous values is retained between cycles to speed the process of checking the energy distribution. Samples usually charge by −4 or −5 V during the beginning of a measurement and do not vary more than 1 V throughout the run.

3.2. Magnetic field determination and centering

The measurement of trace elements at the microgram per gram level implies that the measured count rates at the masses of interest are at most a few counts per second. When count rates are very low it is often not possible to determine the peak positions automatically. Therefore, some other method must be used to determine the magnetic field values for each peak and

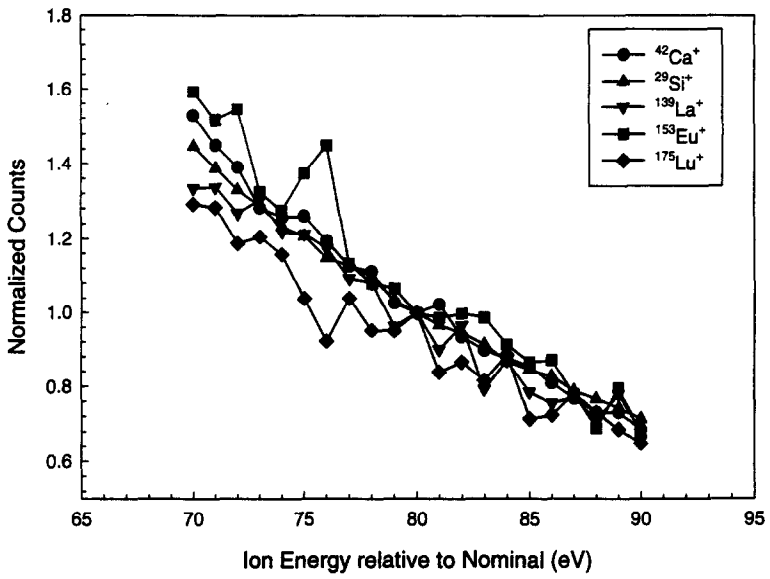

Fig. 2. Expanded view of the energy distributions for several ion species in the region of 80 eV offset (normalized to the value at 80 eV). This is the region in which REE analyses are done. Note that the relative variation as a function of sample offset between curves is small.

to make changes in the values to account for drift in the instrument.

Two methods have been employed for this correction; both work well. Zinner and Crozaz [4] used one of the REEs with a relatively high intensity (usually a light REE), as well as one of the major element signals, to make adjustments to coefficients in a quadratic relation between magnetic field and the apparent mass (obtained from a look-up table). This technique does have the drawback that at least one signal from the REE or in the region of the REE must be large enough to allow automatic centering.

Another method is to use fixed field dispersions from a reference peak, typically chosen to be a major element peak. This method works well for samples in which all the trace elements to be measured have very low abundances. The dispersions can be checked, or calibrated on samples like the National Institute of Standards and Technology (NIST) SRM-610 glass that has ~500 μg/g of the REE and other elements in it. This method was used for the data taken here. Typically, the dispersions are stable for weeks or months. When dispersions are determined, the feedback voltage from the secondary magnet Hall probe is noted for at least one reference peak. If the dispersions require recalibration or must be checked at some later time then the instrument can be retuned so that the previously measured digital to analog converter (DAC) value corresponds to the previous Hall probe voltage when the reference signal peak is passing through the mass spectrometer. When this recalibration is performed the previously determined dispersions will usually be correct. A disadvantage to this method is that when the machine conditions change too drastically, all of the dispersions must be recalibrated.

4. Details of the deconvolution algorithm

The REE, and sometimes Ba and Hf concentrations, are determined by a deconvolution of the energy-filtered ion signals into elemental ion (M^+) and element-oxide ion (MO^+) signals (Cs is usually neglected because its abundance is extremely low in nearly all natural samples). For the deconvolution, count rates are measured at up to 47 masses, typically from 134 to 180 u. There are as many as 27 species involved, Ba to Hf and BaO to ErO. Thus, because there are more equations than unknowns, a least squares fit can be done to determine the elemental

intensities. The masses and species that can be involved in the deconvolution are shown in Table 1. The solution is obtained in three iterations.

The first iteration involves a least squares solution of the equation

$$C_m = \sum_i a_{mi} I_i$$

where C_m = the count rate at mass "m," a_{mi} = a constant that is the natural isotopic abundance of species "i" at mass "m," and I_i = the unknown ion signal count rate of species "i" in c/s. The algorithm does not use a fixed deconvolution matrix a_{mi} but creates the matrix in an adaptive way by reading the raw data file and then selecting items from a list of elements in a second file that have isotopes at the measured masses. Only the species for which masses have been measured that would have a total isotopic abundance above a predetermined limit (currently 1%) are put into the matrix (i.e. isotopes that comprise an abundance of at least 1% of all of the isotopes of a given element must have been measured for that element to be included in the matrix). This "adaptive" method has the advantage of not limiting the analyst to always measuring a fixed set of masses.

To perform a least squares analysis, a χ^2 statistic is formed:

$$\chi^2 = \sum_{m=134}^{180} \frac{\left(C_m - \Sigma_i\, a_{mi} I_i\right)^2}{\sigma_m^2}$$

and minimized (where σ_m is the uncertainty assigned to the measurement of C_m) to produce:

$$I_i = \sum_j b_{ji}^{-1} B_j$$

(b_{ji}^{-1} is an element of the inverse of the b_{ji} matrix) where

$$b_{ji} = \sum_m \frac{a_{mi} a_{mj}}{\sigma_m^2}$$

and

$$B_j = \sum_i b_{ji} I_i$$

The uncertainties of the deconvolved elemental ion intensities, I_i, are given by:

$$\sigma_i = \left[\sum_m \frac{1}{\sigma_m^2} \left(\sum_j b_{ji}^{-1} a_{mj} \right)^2 \right]^{1/2}$$

This first pass iteration gives the elemental ion intensities, I_i, for Ba, La, Pr, Nd, Sm, and Eu but does not compute the heavier REEs very accurately. This is because the lighter REEs are often more abundant than the heavy REEs and the oxides of the light REEs interfere at the masses of the heavy REEs. The uncertainties assigned to each of the count rates (the σ_m) were initially computed from counting statistics by Zinner and Crozaz [4] and others (e.g. see [9]). Later it was discovered that cycle-to-cycle variation in the counts typically exceeded the expected value for counting statistics [13]; thus the error on the mean of the cycle data was used as σ_m.

To constrain the intensities of the heavy REE, Gd to Lu, information about the oxide-to-element ratios, η_i, must be incorporated into the deconvolution. If the ratio of any two η_i is nearly independent of energy, then any variations in the η_i are by approximately a common factor, Φ. Variations may occur because of inhomogeneous sample charging. Known oxide-to-element ratios, η_i, are used, along with the I_i of La, Ce, Pr, Nd, Sm, and Eu computed in the first iteration, to compute the signals from LaO, CeO, PrO, NdO, SmO, and EuO. A column is added to the a_{mi} matrix and the signal at each mass from 155 to 169 from these oxides is placed there. The new B_j and b_{ji} that are computed are sums from 155 to 169 u rather than 134 to 180 u. The I_i are computed again, but only for the heavier REEs from Gd on up and the last I_i is the oxide factor, Φ. The second iteration constrains the I_i of Gd and Tb more tightly than the first. It is important to know the Gd and Tb intensities well so that Yb and Lu, the species at which GdO and TbO interfere, can be accurately calculated.

The third iteration takes the value of Φ computed previously and subtracts directly the computed contributions of SmO, GdO, and TbO to the C_m from 170 to 176 u. The ion signals from 170 to 179 u are then deconvolved into Yb, Lu, Hf, and DyO (ErO is

Table 1
Matrix of species and masses involved in rare earth element abundance deconvolution

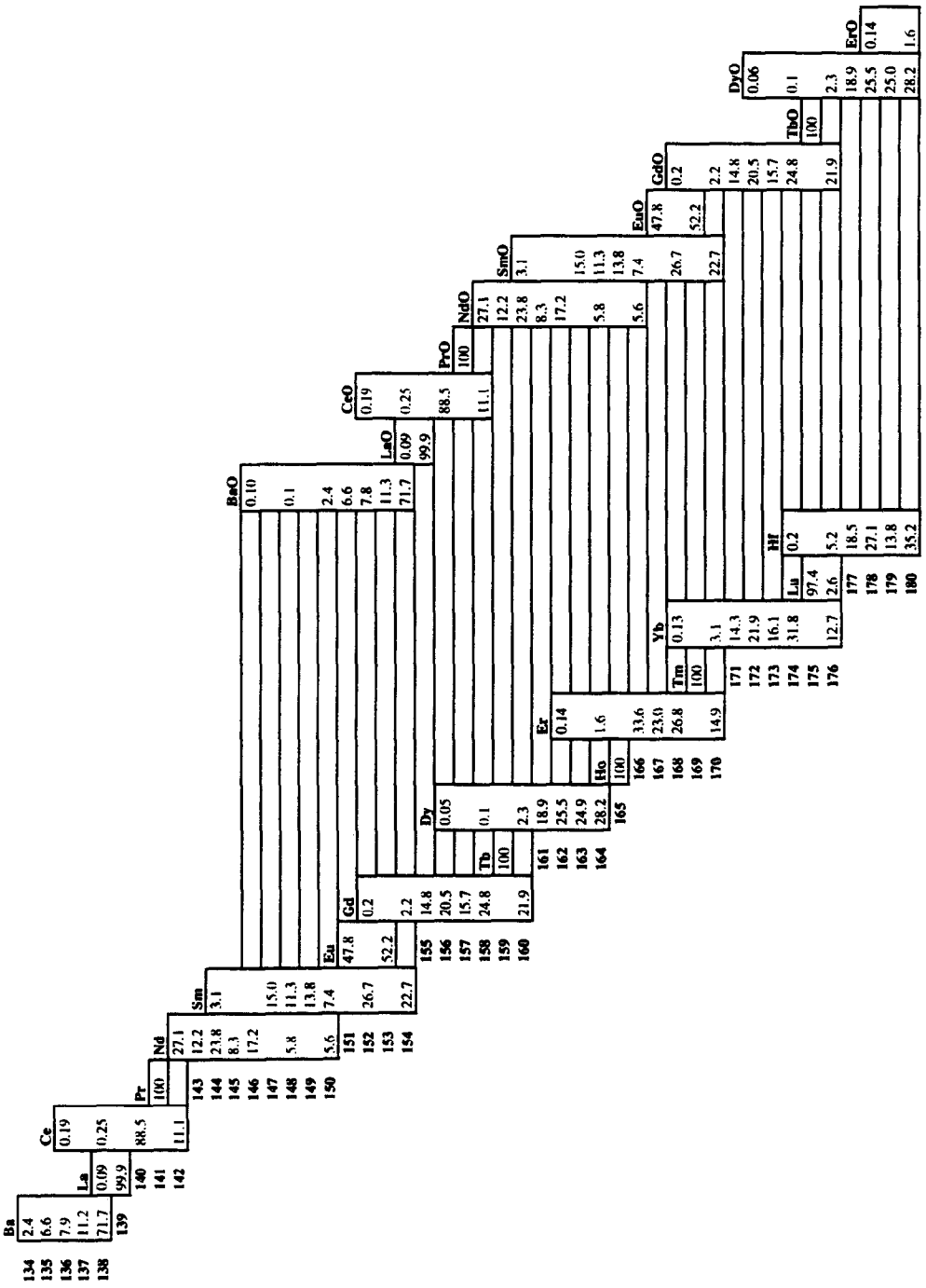

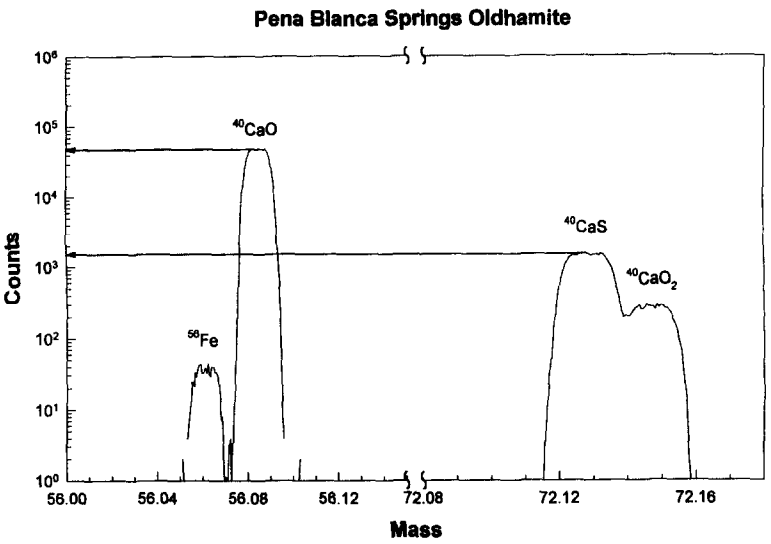

Fig. 3. High resolution mass spectrum around 56 and 72 u showing peaks for $^{40}Ca^{16}O^+$, $^{40}Ca^{32}S^+$, and $^{40}Ca^{16}O_2^+$. The spectra, taken under the same instrumental conditions for the two masses, show that the signal from the sulfide of Ca is more than an order of magnitude lower than the CaO^+ signal.

neglected). When the final value of χ_v^2 (the reduced χ^2) is computed it is generally near unity.

The algorithm provides the individual terms in the sum for χ_v^2 to the user so that the relative contribution for each computed species can be viewed. This allows the user to assess the "goodness" of the determination of individual species.

4.1. Sulfides

The REE abundances can be measured in sulfides as well as oxygen-based minerals. The REEs in meteorites classified as enstatite achondrites are present almost exclusively in the mineral oldhamite (CaS), which does not occur terrestrially. SIMS measurements of the REEs in sulfides from these meteorites have been made by Wheelock et al. [11], Floss and Crozaz [14], and Fahey et al. [15]. An initial concern with measurements in sulfides was the production of REE–sulfide interferences at the heaviest REE from the light REEs. However, a detailed look at the signal present in the region of the REE and REE-sulfides revealed that sulfide ion production was an order of magnitude lower than the oxide production, which is in turn an order of magnitude less intense than the REE ion signal. Fig. 3 illustrates this point by showing the relative intensities of the CaO and CaS ions. Calcium has an ion yield similar to the REE [16]. If REE sulfides behave similarly to CaS, one would expect the REE sulfide contribution to be less than 1% of the heaviest REE ion signals for minerals with nearly "flat" REE abundance patterns.

5. Direct measurements of oxide-to-element ratios

5.1. Sample glasses

To determine the oxide-to-element ratios and their behavior as a function of energy offset, a set of doped Ti-pyroxene composition glasses was made. Each glass nominally contained ~500 μg/g of several REEs chosen so the oxides had no corresponding elemental interferences. In addition to the REEs, ~500 μg/g of Hf, W, and Re was added to the glasses. The nominal major element composition (in weight percent) based on the starting oxides that made up the glass is 25.8% CaO, 18.5% Al_2O_3, 9.8% MgO, 5.4% TiO_2, and 40.2% SiO_2. Four glasses were made to measure oxide-to-element ratios: K3399 with La, Ce, Pr, Nd, Sm, and Eu; K3400 with Gd, Dy, Tb, Er, and Ho; KW3604 containing Tb, Tm, Lu, and Hf; and KW3605 with Hf, W, and Re. Two additional glasses were also produced, one for a blank, with no trace

Table 2
Oxide-to-element ratios for the rare earth element and Hf, W, and Re

Offset voltage	La	Ce	Pr	Nd	Sm	Eu
−40	0.394 ± 0.003	0.441 ± 0.003	0.355 ± 0.003	0.312 ± 0.014	0.192 ± 0.008	0.114 ± 0.001
−60	0.246 ± 0.004	0.274 ± 0.004	0.218 ± 0.003	0.189 ± 0.009	0.107 ± 0.005	0.069 ± 0.004
−80	0.153 ± 0.001	0.173 ± 0.008	0.132 ± 0.005	0.110 ± 0.017	0.069 ± 0.011	0.044 ± 0.002
−100	0.105 ± 0.004	0.103 ± 0.005	0.096 ± 0.004	0.085 ± 0.005	0.047 ± 0.006	0.035 ± 0.003
−120	0.069 ± 0.005	0.074 ± 0.005	0.070 ± 0.005	0.064 ± 0.009	0.028 ± 0.006	0.021 ± 0.002
Fahey et al.	0.158	0.195	0.141	0.121	0.065	0.048

Offset voltage	Gd	Dy	Tb	Er	Ho
−60	0.180 ± 0.006	0.131 ± 0.003	0.171 ± 0.001	0.135 ± 0.006	0.132 ± 0.001
−80	0.106 ± 0.009	0.076 ± 0.009	0.094 ± 0.009	0.073 ± 0.006	0.074 ± 0.004
−100	0.063 ± 0.010	0.053 ± 0.001	0.066 ± 0.001	0.055 ± 0.003	0.053 ± 0.001
−120	0.045 ± 0.011	0.033 ± 0.002	0.047 ± 0.002	0.031 ± 0.000	0.034 ± 0.001
Fahey et al.	0.103	0.065	0.096	0.066	0.064

Offset voltage	Yb	Tm	Lu	Hf	Hf	W	Re
−40	0.157 ± 0.009	0.193 ± 0.001	0.274 ± 0.002	0.709 ± 0.007	0.673 ± 0.010	1.421 ± 0.064	0.315 ± 0.082
−60	0.084 ± 0.000	0.111 ± 0.001	0.149 ± 0.002	0.376 ± 0.005	0.364 ± 0.010	0.740 ± 0.047	0.237 ± 0.015
−80	0.050 ± 0.006	0.064 ± 0.003	0.089 ± 0.006	0.205 ± 0.019	0.194 ± 0.011	0.394 ± 0.016	0.153 ± 0.039
−100	0.036 ± 0.006	0.043 ± 0.002	0.060 ± 0.002	0.112 ± 0.011	0.112 ± 0.023	0.233 ± 0.022	0.112 ± 0.002
−120	0.022 ± 0.003	0.032 ± 0.002	0.041 ± 0.002	0.076 ± 0.008	0.083 ± 0.018	0.130 ± 0.025	0.097 ± 0.003
Fahey et al.	0.047	0.052	0.067				

elements added, and a composite glass, KW3610, with all the trace elements used in the previous four glasses at a level of ~500 μg/g.

5.2. Data

The oxide-to-element ratios, η_i, for all of the measured elements as a function of ion energy are given in Table 2. Values are also shown from the work of Fahey et al. [9] taken at an offset of 100 eV from the 10% edge of the distribution. The data plotted in Fig. 4 were fit to a second order polynomial for each element. The second order fit appears to be a reasonable representation of the behavior of the data. The η_i vary by 10% to 20% over a span of ~10 eV around 80 eV (Fig. 4), indicating that small errors from sample charging have little effect on these ratios, and hence on the outcome of the analysis. The data reported here are in reasonably good agreement with those given by Fahey et al. [9].

The use of an added column in the deconvolution matrix for the second pass of the analysis algorithm and the use of an "oxide factor" in the third pass depend upon the ratios of the η_i being approximately independent of energy. Fig. 5 shows the ratios of the η_i for Ce and Tm relative to that for La. The values are constant to within 1 standard deviation about the mean. The effect of these variations is small compared with typical counting statistical errors for REE measurements.

6. Quantification and sensitivity factors

6.1. Method

Conversion of the ion intensities generated by the REE ion signal deconvolution into abundances is done via the formula:

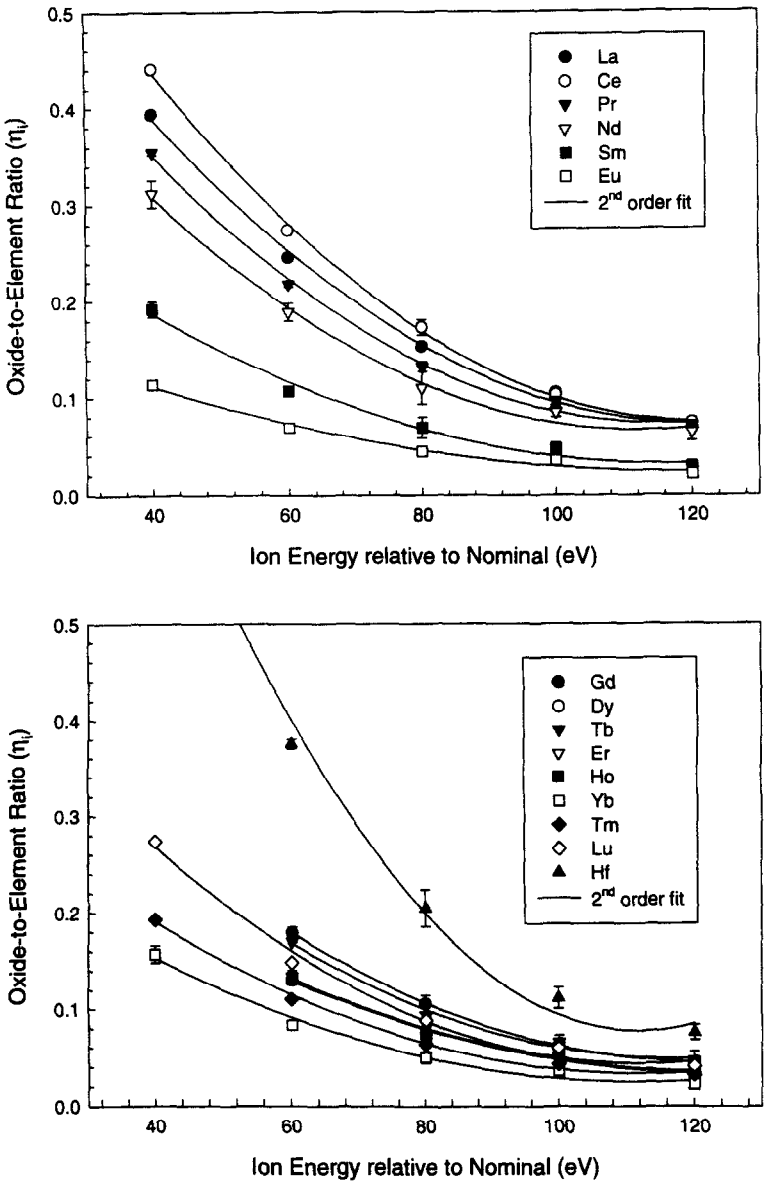

Fig. 4. Direct measurements of the oxide-to-element ratios for the REE and Hf are plotted as a function of energy. The trend for each of the curves is approximately quadratic.

$$[\mathrm{REE}]_i = F_i^M \frac{\mathrm{REE}_i^+}{M^+} [MC]$$

where M is some major element cation like Ca, Ti, or Si, $[MC]$ is a known concentration of a species in the sample (e.g. CaO, SiO_2, or Ca), and F_i^M is the sensitivity factor for REE "i" with respect to the cation "M."

6.2. Data

Measured concentrations of the REEs for the NIST SRM-600 series glasses are given in Table 3. NIST SRM-610 glass was used as the reference material from which the sensitivity factors were obtained. The assumed concentrations for NIST SRM-610 listed in

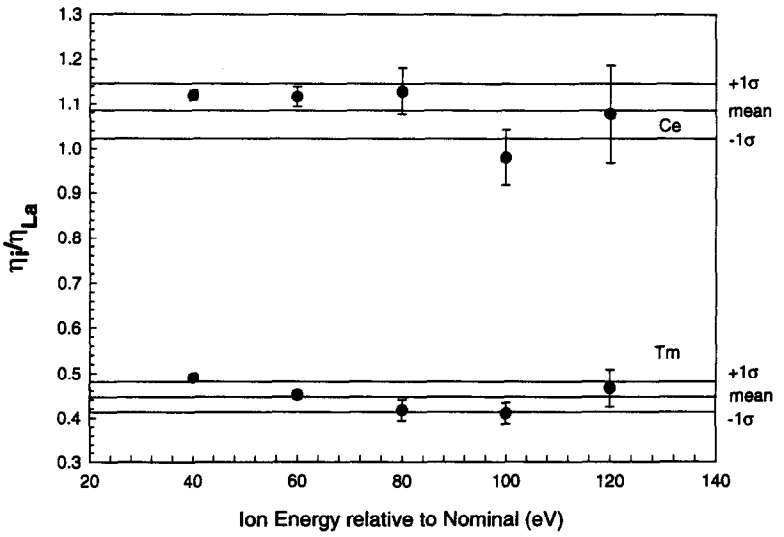

Fig. 5. The small variation in the ratio of the η_i shows that it is a good approximation to adjust the oxide-to-element ratios by a constant factor during the REE signal deconvolution. The lines drawn in the figure represent the means of each set and one standard deviation from the mean.

the fourth column of Table 3 are a compilation of reported concentrations measured in NIST SRM-610 [17]. The sensitivity factors obtained in this way were then used to compute the concentrations for NIST SRM-612, 614, and 616. Clearly, the compilation of concentrations for the NIST SRM-612 glass is not completely consistent with the sensitivity factors obtained on the NIST SRM-610 glass, with some deviations being over 10% and an overall average deviation of −5.7%. Data for NIST SRM-614 show that the concentration of all of the REE down to ~0.5 μg/g can be measured with this technique under these measurement conditions when all of the REE abundances are similar. The data from both NIST SRM-614 and NIST SRM-616 indicate that the detection limit for the REE under these conditions is ~100 ng/g. In NIST SRM-616 the REE concentrations are below this level, and the data are therefore inconclusive.

6.3. Artifacts

Concentrations of the REE, Ba, and Hf for three of the Ti-pyroxene glasses made for this study are shown in Table 4. The least squares fits to the data are reasonably good as evidenced by the reduced-χ^2 values, and each glass has approximately the nominal concentration of 500 μg/g for the REE intentionally added. However, some small artifacts of the fitting process are evident in these measurements. The data for RG3399 show a significant contribution at Gd and Er and negative concentrations at Tb and Ho. These artifacts are due to the improper oxide corrections at these masses and indicate the level to which these concentrations can be measured in the presence of much higher concentrations of the lighter REE. Table 1 shows that Gd has interferences from BaO, LaO, CeO, PrO, NdO, and SmO, and the data for RG3399 in Table 4 indicate that a ratio of ~100:1 of any of these light REE to Gd is about the limit above which one can expect incorrect concentrations. Similarly, the data from RG3400 show significant apparent concentrations for Yb, Lu, and Hf. These artifacts are also due to incomplete corrections for oxides of lighter elements. Although these samples represent extreme concentration variations that may never, or rarely, be found in nature they illustrate the appearance of potential artifacts.

6.4. Sensitivity factors and variations between laboratories

There is a different set of F_i^M for each material or set of materials. The procedure followed for the best

Table 3
Concentrations of the rare earth element and Hf in National Institute of Standards and Technology SRM-600 series glasses (μg/g)

	NIST SRM-610[a]		Assumed	NIST SRM-612[b]		Computed		NIST SRM-614[c]	NIST SRM-616[d]	
	Run A	Run B	concentration	Run A	Run B	concentration	Δ^5	Run B	Run A	Run B
La	435.25 ± 2.77	438.08 ± 2.84	436.6	33.65 ± 0.81	33.50 ± 0.81	35.49	−5.4%	0.64 ± 0.11	0.04 ± 0.03	0.02 ± 0.02
Ce	444.28 ± 3.06	443.91 ± 3.12	443.3	35.87 ± 0.90	35.02 ± 0.90	38.24	−7.3%	0.55 ± 0.11	0.58 ± 0.45	
Pr	428.90 ± 2.75	431.32 ± 2.82	431.2	35.65 ± 0.83	33.51 ± 0.81	37.06	−6.7%	0.97 ± 0.13		
Nd	423.93 ± 3.08	434.18 ± 3.17	430.0	33.34 ± 0.90	35.02 ± 0.93	34.95	−2.2%	0.54 ± 0.11	0.25 ± 0.08	0.12 ± 0.12
Sm	451.74 ± 3.99	446.10 ± 4.06	456.6	35.37 ± 1.17	34.43 ± 1.16	36.37	−4.1%	0.66 ± 0.16	0.25 ± 0.18	0.11 ± 0.20
Eu	427.86 ± 2.62	430.51 ± 2.69	429.5	32.44 ± 0.76	31.22 ± 0.74	34.59	−8.0%	0.61 ± 0.10		0.04 ± 0.28
Gd	425.53 ± 5.37	426.97 ± 5.50	422.9	35.99 ± 1.60	32.85 ± 1.60	37.09	−7.2%	0.66 ± 0.18	0.08 ± 0.09	0.11 ± 0.06
Tb	439.51 ± 2.92	450.19 ± 3.02	446.0	36.12 ± 0.87	34.99 ± 0.87	36.29	−2.0%	0.60 ± 0.11	0.04 ± 0.03	0.04 ± 0.03
Dy	431.90 ± 3.06	434.88 ± 3.14	434.8	32.29 ± 0.87	34.09 ± 0.91	35.66	−6.9%	0.59 ± 0.11	0.09 ± 0.09	0.08 ± 0.08
Ho	448.41 ± 3.03	457.63 ± 3.13	453.0	38.16 ± 0.92	35.44 ± 0.89	37.89	−2.9%	0.55 ± 0.11	0.02 ± 0.02	
Er	429.97 ± 3.43	436.08 ± 3.53	434.7	34.01 ± 1.00	34.82 ± 1.03	37.98	−9.4%	0.59 ± 0.13	0.08 ± 0.08	
Tm	425.67 ± 3.00	421.97 ± 3.06	422.5	34.96 ± 0.90	34.93 ± 0.91	37.66	−7.2%	0.68 ± 0.12		
Yb	459.30 ± 3.48	455.21 ± 3.54	462.7	36.44 ± 1.03	34.31 ± 1.01	39.51	10.5%	0.67 ± 0.13		
Lu	431.82 ± 3.61	427.18 ± 3.69	433.1	35.10 ± 1.08	31.72 ± 1.04	37.57	−11.1%	0.48 ± 0.12		
Hf	410.42 ± 15.3	409.17 ± 15.5	411.2	33.13 ± 4.28	39.73 ± 4.44	34.77	4.8%	0.11 ± 0.69		
Δ_{ave}							−5.7%			
Φ	0.99	1.00		0.92	1.07			0.81	NPC	NPC
χ^2_ν	5.7	5.3		0.98	1.03			1.31	NPC	NPC

[a]Nominal concentration of REE in NIST 610 glass is 500 μg/g.
[b]Nominal concentration of REE in NIST 612 glass is 50 μg/g.
[c]Nominal concentration of REE in NIST 614 glass is 1 μg/g.
[d]Nominal concentration of REE in NIST 616 glass is 50 ng/g.
[e]Deviation of the computed concentration relative to those given in I. Hutchinson, personal communication.
Key: NIST, National Institute of Standards and Technology; NPC, not properly computed; REE, rare earth element.

Table 4
Concentrations of rare earth element, Ba, and Hf in Ti-pyroxene test glasses

	RG3399	RG3400	KW3604
Ba	12.44 ± 0.94	14.96 ± 0.45	15.67 ± 0.49
La	577.99 ± 5.08	0.43 ± 0.06	0.47 ± 0.08
Ce	578.96 ± 5.54	0.93 ± 0.10	0.75 ± 0.10
Pr	529.00 ± 4.86	0.11 ± 0.04	0.13 ± 0.04
Nd	522.12 ± 5.45	0.21 ± 0.06	0.16 ± 0.05
Sm	549.05 ± 6.99	0.12 ± 0.07	0.05 ± 0.05
Eu	510.34 ± 4.53	0.34 ± 0.10	0.02 ± 0.03
Gd	6.63 ± 3.59	673.19 ± 3.71	0.07 ± 0.06
Tb	−1.04 ± 0.58	714.63 ± 2.77	ND
Dy	0.10 ± 1.33	735.87 ± 2.86	0.12 ± 0.04
Ho	−0.66 ± 0.56	740.35 ± 2.89	ND
Er	2.37 ± 1.58	711.76 ± 3.11	0.13 ± 0.05
Tm	0.44 ± 0.93	0.25 ± 0.12	693.85 ± 3.04
Yb	ND	7.77 ± 1.12	727.40 ± 3.33
Lu	ND	6.47 ± 1.23	710.88 ± 3.53
Hf	ND	22.77 ± 6.56	644.08 ± 13.96
F	0.99	1.00[a]	0.83
χ^2_v	2.08	3.29	2.36

Stated errors are 1 σ_{mean}.
[a]Oxide factor forced to unity in this case.
Key: ND, not determined.

quantitative measurements by SIMS is akin to procedures followed in quantitative electron microprobe x-ray analysis. It involves 1) the measurement of a reference sample with known REE trace concentrations and of similar major element composition before measurement of the unknowns; 2) the F_i^M are checked with the reference sample and adjusted if need be; 3) the unknown is measured; and 4) the reference sample is remeasured to monitor any changes in conditions during the set of measurements.

The F_i^M do vary with measurement conditions and result in a 20% relative uncertainty among the REE without calibration. The absolute uncertainty will be larger. The sensitivity factors obtained for silicate minerals with respect to SiO_2, normalized to the value for La, are shown in Fig. 6. The values were taken with three different instruments, one at Washington University in St. Louis, another at The California Institute of Technology (Caltech), and the final one at NIST in Gaithersburg. The first two were obtained with a 75-μm imaged field configuration, whereas the NIST data were obtained with a 150-μm imaged field. The absolute value for the $F^{Si}_{L,a}$ from each laboratory is 0.92 from Washington University, 0.80 from Caltech, and 1.5 from NIST. The large difference between the NIST value and the others is almost certainly because of the different imaged field used, which tends to change the relative sensitivities of elements.

The lack of a standard with a known and accepted REE composition makes it difficult to compare data

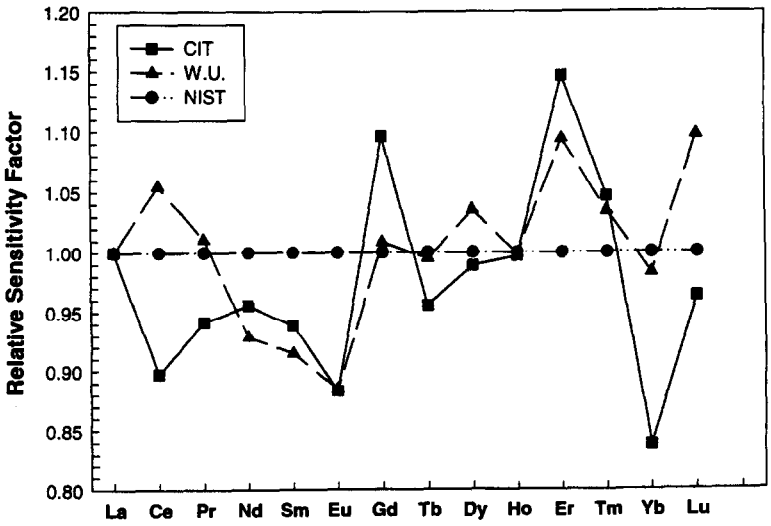

Fig. 6. Variation in the doubly normalized sensitivity factors for the REE from three laboratories is plotted. The maximum variation among laboratories is ~15%.

Table 5
Sensitivity factors normalized to La

	Silicate SiO_2	Silicate CaO	Sulfide Ca
La	≡1.00	≡1.00	≡1.00
Ce	1.08	0.97	1.25
Pr	1.00	0.94	0.87
Nd	1.01	0.96	0.79
Sm	0.94	0.88	0.74
Eu	0.88	0.78	0.61
Gd	0.96	1.05	1.13
Tb	1.08	1.03	1.38
Dy	1.08	1.07	1.03
Ho	1.14	1.14	1.07
Er	1.14	1.31	1.50
Tm	1.16	1.21	1.52
Yb	1.27	1.07	1.41
Lu	1.48	1.42	2.05

for sensitivity factors from different laboratories and instruments, because none of the laboratories measuring REE by SIMS use the same material to obtain their sensitivity factors. In addition, the uncertainty to which the REE abundances are known in materials typically used as standards is generally worse than the counting error attainable via SIMS. Thus, the uncertainty of compositions measured with SIMS is limited by the uncertainty level to which the reference sample compositions are known.

Three sets of normalized sensitivity factors are given in Table 5. The same data are plotted in Fig. 7. The first column in Table 5 contains the relative sensitivity factors with respect to SiO_2 derived from NIST SRM-610 glass measurements and are the values used in this study. The second column in Table 5 contains values obtained from measurements on a different Ti-pyroxene glass on the Caltech ims-3f. These two data sets should be nearly identical; thus, the observed deviations are representative of the magnitude of variation between labs, just as in Fig. 6.

Sensitivity factors for REE measured in CaS are also given in Table 5 and shown in Fig. 7. The factors for this sulfide mineral were obtained by comparison with instrumental neutron activation analysis data on an aliquot of oldhamite from the Pena Blanca Spring Aubrite [18]. The sensitivity factors for sulfide minerals exhibit greater variation than those for the silicate minerals.

7. Conclusions and future work

The algorithm presented here is capable of deconvolving measured ion signals into REE and REE oxide ion signals. The presence of oxide interferences

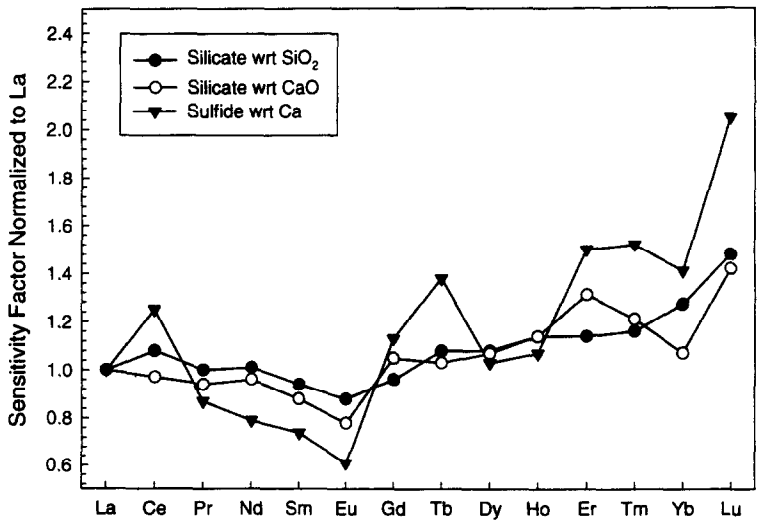

Fig. 7. Plot of the doubly normalized sensitivity factors for silicate and sulfide. The variation in the sulfide sensitivity factors is significantly larger than for silicate.

is accounted for by direct deconvolution and by the use of measured oxide-to-element ratios. These ratios are relatively insensitive to ion energy and all scale by approximately a common factor under changing charging conditions.

The abundances of REE and other trace elements can be measured in a variety of materials provided appropriate references or standards are available. Sensitivity factors should be checked and calibrated before each measurement because 10% to 20% relative variations can occur without this calibration. Absolute abundance uncertainties can be even larger.

The lack of well characterized reference materials is a limitation for the measurement of REE abundances in minerals if uncertainties lower than ~10% to 20% are required. Further work to characterize the glasses synthesized for this work may provide at least a partial solution to this problem. However, measurements and characterization of large varieties of other materials must also be done to provide a significant base of references upon which to draw.

Acknowledgements

The author would like to thank the anonymous reviewer for thoughtful and helpful comments. Eric Windsor and Douglas Blackburn skillfully produced the Ti-pyroxene glasses for this study in the NIST glass fabrication laboratory. Dr. Katherina Lodders provided the oldhamite sample and many helpful discussions. Thanks to Dr. Gary Huss and all the other Lunatics at Caltech for their help in making the measurements there. C-source code for the REE deconvolution and quantitation as well as data files and future refinements of concentration measurements in the various glasses are available via the Internet by sending e-mail to the author at albert.fahey@nist.gov

References

[1] N. Shimizu, M.P. Semet, C.J. Allegre, Geochim. Cosmochim. Acta. 42 (1978) 1321.
[2] J.B. Metson, G.M. Bancroft, H.W. Nesbitt, R.G. Jonassen, Nature 307 (1984) 347.
[3] S.J.B. Reed, Int. J. Mass Spectrom. Ion Processes 54 (1983) 31.
[4] E. Zinner, G. Crozaz, Int. J. Mass Spectrom. Ion Processes 69 (1986) 17.
[5] T. Ireland, Adv. Anal. Geochem. 2 (1995) 1.
[6] L. Ottolini, P. Bottazzi, R. Vannucci, Terra Abstracts 3 (1991) 461.
[7] P. Bottazzi, L. Ottolini, R. Vannucci, GeoStandards Newsletter 15 (1991) 51.
[8] S. Meloni, M. Oddone, P. Bottazzi, L. Ottolini, R. Vannucci, J. Radioanal. Nucl. Chem. 168 (1993) 115.
[9] A. Fahey, J. Goswami, K. McKeegan, E. Zinner, Geochim. Cosmochim. Acta 51 (1987) 329.
[10] A. Fahey, E. Zinner, G. Crozaz, A. Kornacki, Geochim. Cosmochim. Acta 51 (1987) 3215.
[11] M.M. Wheelock, K. Keil, C. Floss, G.J. Taylor, G. Crozaz, Geochim. Cosmochim. Acta 58 (1994) 449.
[12] G.N. Hanson, Annu. Rev. Earth Planet. Sci. 8 (1980) 371.
[13] I. Hutcheon, personal communication, 1993.
[14] C. Floss, G. Crozaz, Geochim. Cosmochim. Acta. 57 (1993) 4039.
[15] A. Fahey, G. Huss, G. Wasserburg, K. Lodders, Lunar Planet. Sci. XXVI (1995) 385.
[16] R. Hinton, Chem. Geo. 83 (1990) 11.
[17] N.J.G. Pearce, W.T. Perkins, J.A. Westgate, M.P. Gorton, S.E. Jackson, C.R. Neal, S.P. Chenery, Geostand. Newsl. 21 (1997) 115.
[18] K. Lodders, H. Palme, F. Wlotzka, Meteoritics 28 (1993) 538.